

Oscillatory convective modes in red giants: a possible explanation of the long secondary periods

Hideyuki Saio,¹ Peter R. Wood² Masaki Takayama^{1,3}, and Yoshifusa Ita¹

¹*Astronomical Institute, Graduate School of Science, Tohoku University, Sendai, Miyagi 980-8578, Japan*

²*Research School of Astronomy and Astrophysics, Australian National University, Cotter Road, Weston Creek, ACT 2611, Australia*

³*Department of Astronomy, School of Science, The University of Tokyo, Bunkyo-ku, Tokyo 113-0033, Japan*

14 July 2015

ABSTRACT

We discuss properties of oscillatory convective modes in low-mass red giants, and compare them with observed properties of the long secondary periods (LSPs) of semi-regular red giant variables. Oscillatory convective modes are very nonadiabatic g^- modes and they are present in luminous stars, such as red giants with $\log L/L_\odot \gtrsim 3$. Finite amplitudes for these modes are confined to the outermost nonadiabatic layers, where the radiative energy flux is more important than the convective energy flux. The periods of oscillatory convection modes increase with luminosity, and the growth times are comparable to the oscillation periods. The LSPs of red giants in the Large Magellanic Cloud (LMC) are observed to lie on a distinct period-luminosity sequence called sequence D. This sequence D period-luminosity relation is roughly consistent with the predictions for dipole oscillatory convective modes in AGB models if we adopt a mixing length of 1.2 pressure scale height ($\alpha = 1.2$). However, the effective temperature of the red-giant sequence of the LMC is consistent to models with $\alpha = 1.9$, which predict periods too short by a factor of two.

Key words: convection – stars: AGB and post-AGB – stars: late-type – stars: low mass – stars: oscillations .

1 INTRODUCTION

Long period variables (LPVs) are red giant stars which are known to obey several period-luminosity relations (e.g., Wood et al. 1999; Kiss & Bedding 2003; Ita et al. 2004; Soszyński et al. 2004, 2007). Among these relations, the so-called sequence D relation corresponds to the longest period for a given luminosity, with periods ranging from about 200 d to 1,500 d. This period is actually a long secondary period (LSP) co-existing with a primary period which is about 8 times shorter and which typically falls on sequence B (e.g., Wood et al. 1999). Although other sequences (except for sequence E) are generally associated with radial or nonradial pulsations (Wood et al. 1999; Dziembowski & Soszyński 2010; Takayama, Saio & Ita 2013; Mosser et al. 2013; Wood 2015), the origin of sequence D is unknown. Since the discovery of sequence D by Wood et al. (1999), its properties and origin have been discussed widely (e.g., Wood, Olivier & Kawaler 2004; Soszyński et al. 2007; Nicholls et al. 2009). Various models have been considered such as semi-detached binaries (Wood et al. 1999; Soszyński et al. 2007), rotating spots with dust formation (Takayama, Wood & Ita 2015), and radial and nonradial pulsation (Wood et al. 1999). However, none of them give a consistent explanation for the LSP variations.

There is considerable evidence that radial pulsation is not the main mechanism associated with the LSPs. The observed radial velocity variations of a few km s^{-1} (Wood, Olivier & Kawaler 2004; Nicholls et al. 2009), combined with the long periods, would produce a large fractional radius change if the LSP is caused by radial pulsation. However, there is no direct evidence, for example from changes in effective temperature, for a large radius change (Nicholls et al. 2009). In addition, no change in the primary period of the star is observed as might be expected if the radius is changing significantly with the LSP variation (Wood, Olivier & Kawaler 2004). Finally, we note that the fundamental mode radial pulsation period of models is much shorter than the LSP (e.g. Wood et al. 1999). All these factors indicate that the LSPs are not caused by radial pulsation.

One previous suggestion has associated convection with LSPs in red giants. Stothers (2010) considered giant convection cells for the origin of the LSPs. He argued that the turnover time of giant convection cells is comparable with observed length of LSPs, and that the observed radial velocity changes can be interpreted as convection motion, which causes no radius change. However, it is not clear why the

turnover time would be related to a distinct periodicity with a light amplitude of up to one magnitude.

In this paper we discuss oscillatory convective modes in red giants. They are oscillations confined to the outermost layers of the deep envelope convection. Dipole oscillatory convective modes have properties favorable for the cause of the LSPs, such as periods longer than the fundamental radial mode and small temperature variations. We also note that the above mentioned difficulties in radial pulsations associated with the observed radial velocity variations of LSPs are not applicable for a dipole mode pulsation because it does not change mean stellar radius.

We discuss evolutionary models on which we performed pulsation analysis in Section 2. The properties of the oscillatory convective modes are discussed in Section 3. We make comparisons with observations of LSP variability in Section 4.

2 MODELS

Fig. 1 is a HR diagram showing the positions of sequence D stars (small dots), and some evolutionary tracks on the red-giant branch and asymptotic giant branch (AGB) for initial masses of 1.0, 1.3, and 2.0 M_{\odot} with $\alpha = 1.9$ and 1.2, where α , a mixing-length parameter, is defined as the mixing-length divided by the pressure scale-height. Sequence D stars are adopted from OGLE III identification by (Soszyński et al. 2009). The luminosity and effective temperatures were obtained from 2MASS photometry data of J and K (Skrutskie et al. 2006) and the temperature and bolometric correction - color relations by Houdashelt et al. (2000) and Houdashelt, Bell & Sweigart (2000), and a distance modulus of 18.54 mag (Keller & Wood 2006) of the Large Magellanic Cloud (LMC). The 2MASS J, K magnitudes were converted to the CIT system using the relation derived by Carpenter (2001).

Stellar evolution models were obtained using the MESA (Modules for Experiments in Stellar Astrophysics; version 7184) code (Paxton et al. 2013). The hydrogen and metal abundances adopted are $(X, Z) = (0.73, 0.008)$. Models of various initial masses ranging from 0.9 M_{\odot} to 2.0 M_{\odot} were computed with several values (between 1.0 and 1.9) of the mixing-length parameter α .

The central helium flashes start to occur near the tip of the red giant branch (RGB) at $\log L/L_{\odot} \approx 3.3$. After a few shell flashes, the star transits to a steady central helium burning around $\log L/L_{\odot} \sim 2$. After central helium exhaustion, the evolution along the asymptotic giant branch (AGB) starts. Here helium shell flashes (thermal pulses) occur in which the luminosity changes cyclically while the average luminosity increases gradually. The evolution calculations were stopped when each model reaches at $\log L/L_{\odot} \approx 4.0$. Wind mass loss rate of de Jager, Nieuwenhuijzen & van der Hucht (1988) was included in the calculations.

The majority of the sequence D stars are AGB stars, whose loci on the HR diagram look consistent with evolution models with $\alpha = 1.9$.

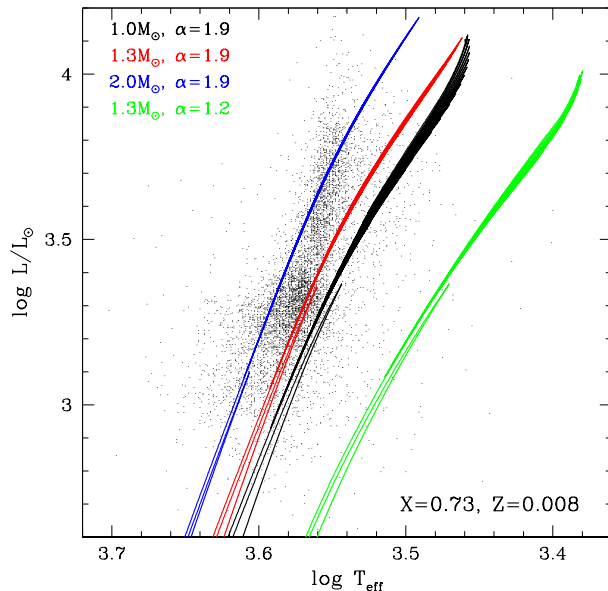


Figure 1. Selected evolutionary tracks computed by the MESA code for initial masses of 1.0 M_{\odot} , 1.3 M_{\odot} and 2.0 M_{\odot} with the mixing-length parameter, $\alpha = 1.9$ and 1.2. The evolutions were started at a pre-main sequence model and calculated through the thermal pulsing AGB stage up to $\log L/L_{\odot} \approx 4.0$. Small dots are sequence D stars identified by Soszyński et al. (2009) (OGLE III).

3 OSCILLATORY CONVECTIVE MODES IN RED GIANTS

Shibahashi & Osaki (1981) discovered that nonradial g^- modes, whose frequencies are purely imaginary (meaning monotonic growth or decay) in the adiabatic condition, corresponding to the convective instability, become oscillatory in extremely nonadiabatic condition. We call them oscillatory convective modes. They are highly unstable (or strongly excited) with growth time comparable with the period. Shibahashi & Osaki (1981) discovered the oscillatory convective modes in studying nonradial pulsations of high angular degrees $\ell \gtrsim 10$ in luminous ($10^5 L_{\odot}$) models hotter than the cepheid instability strip. Such high degree modes are not expected to be observable because of cancellation on the surface. Thirty years later, Saio (2011) found low degree $\ell \lesssim 2$ examples of these oscillatory convective modes in hot massive stars where convection zones are associated with the Fe opacity peak at $T \sim 2 \times 10^5$ K.

In this paper we consider oscillatory convective modes in luminous red giants having deep convection envelopes. Frequencies and amplitude distributions in the stellar interior were obtained by the method described in Saio & Cox (1980), in which the Lagrangian perturbation for the divergence of convective flux is neglected (i.e., $\delta \nabla \cdot F_{\text{conv}} = 0$). The temporal variation is expressed as $\exp(i\sigma t)$ with complex angular frequency σ , so that an oscillation mode is excited (or overstable) if $\sigma_i < 0$, where σ_i is the imaginary part of σ . To represent the value of eigenfrequency, we use normalized (non-dimensional) eigenfrequency ω defined as

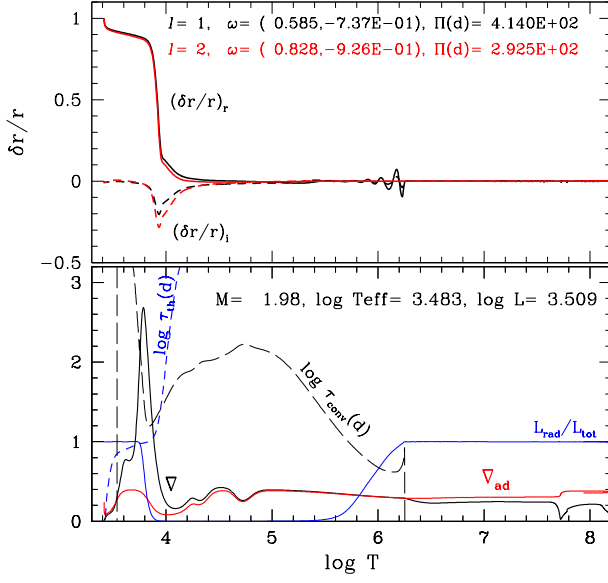


Figure 2. **Top panel:** Amplitude distributions of typical oscillatory convective modes of $\ell = 1$ (black lines) and $\ell = 2$ (red lines) are shown as a function of $\log T$ in a model on the AGB branch for a initial mass of $2.0 M_{\odot}$ with a mixing-length parameter of $\alpha = 1.2$. Solid and dashed lines are, respectively, the real and imaginary parts of the normalized radial displacement $\delta r/r$. The real and imaginary parts of the normalized angular frequency ω and the period Π in days for each mode are shown. We adopt in this paper the convention that a pulsation mode is excited if the imaginary part is negative (i.e., $\omega_i < 0$). **Bottom panel:** Some physical variables in the AGB model are shown, where τ_{conv} and τ_{th} are, respectively, convective turn-over time and thermal time in units of days.

$$\omega = \sigma \sqrt{\frac{R^3}{GM}}, \quad (1)$$

where R , M , and G are stellar radius and mass, and gravitational constant, respectively i.e., the pulsation frequency is normalized by the Kepler frequency at the stellar surface.

The top panel of Fig. 2 shows the amplitude of the radial displacement $\delta r/r$ for oscillatory convective modes of $\ell = 1$ (black lines) and 2 (red lines) in the interior of an AGB model of an initial mass of $2.0 M_{\odot}$ at $\log L/L_{\odot} = 3.5$ with $\alpha = 1.2$. Solid and dashed lines are, respectively, real and imaginary parts of the radial displacement. Actual radial displacement is given by the real part of $\delta r e^{i\sigma t} Y_{\ell}^m(\theta, \phi)$ where $Y_{\ell}^m(\theta, \phi)$ is a spherical harmonic and θ and ϕ are the co-latitude and azimuthal angle, respectively.

The amplitude distributions are remarkably similar for the $\ell = 1$ and 2 modes. Finite amplitudes are mostly confined to the outer layers where the superadiabatic temperature gradient $\nabla - \nabla_{\text{ad}}$ is large and the thermal time τ_{th} is shorter than the periods, indicating that the oscillatory convective modes are very nonadiabatic. Here, ∇ and ∇_{ad} are defined as

$$\nabla = \frac{d \ln T}{d \ln P}, \quad \nabla_{\text{ad}} = \left(\frac{\partial \ln T}{\partial \ln P} \right)_s, \quad (2)$$

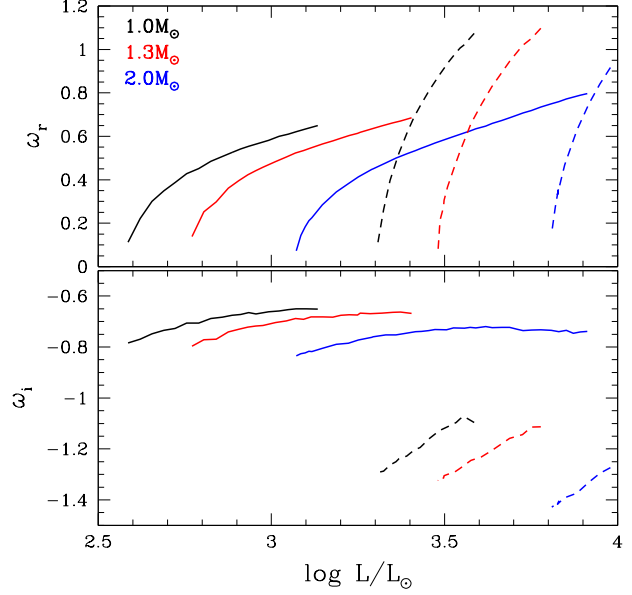


Figure 3. Real (upper panel) and imaginary (lower panel) of normalized eigenvalue of oscillatory convective modes in AGB (non-flashing) models of each mass (black lines – $1.0 M_{\odot}$; red lines – $1.3 M_{\odot}$; blue lines – $2.0 M_{\odot}$). Solid and dashed lines are for models with $\alpha = 1.2$ and 1.9 , respectively.

where P and S are the pressure and the specific entropy, respectively. The thermal time τ_{th} is defined as

$$\tau_{\text{th}} = \frac{(M - M_r) C_p T}{L_r}, \quad (3)$$

where M_r is the mass within the sphere of radius r (i.e., $M - M_r$ is the mass above the sphere of radius r), C_p is the specific heat at constant pressure, and L_r is the local luminosity at radius r .

Also shown in the bottom panel of Fig. 2 is the local convective turnover time defined as

$$\tau_{\text{conv}} = \frac{\alpha H_p}{v_{\text{conv}}}, \quad (4)$$

where H_p is the pressure scale height, and v_{conv} is convective velocity obtained from the mixing-length theory. Note that τ_{conv} decreases toward the inner boundary at $\log T \approx 6.2$; this is because the fractional radius of the convective inner boundary is very small ($r/R \approx 0.006$, while $M_r/M \approx 0.28$). Fig. 2 indicates that in a considerable fraction of the zone where the radial displacement has a large amplitude, τ_{conv} is much larger than the period and most of the energy is carried by radiation (i.e., $L_{\text{rad}}/L_{\text{tot}} \approx 1$). This means that our approximation neglecting the divergence of convective flux is likely to be reasonably good.

The absolute value of the imaginary part of the non-dimensional eigenfrequency ω is comparable with the real part, indicating that the growth time is comparable with the pulsation period. In other words, the oscillatory convective modes are violently excited so that they should be capable of causing semi-regular light/velocity variations of the size observed (e.g., Wood et al. 1999; Soszyński et al. 2004) during LSP variations.

Fig. 3 shows the real part (ω_r ; upper panel) and imagi-

nary part (ω_i ; lower panel) of normalized eigenfrequencies of oscillatory convective modes as a function of the luminosity of AGB models of various masses and with mixing-length parameters $\alpha = 1.2$ (solid lines) and 1.9 (dashed lines). (We have selected only non-flashing, i.e., slowly evolving, AGB models.) Generally, ω_r increases and $|\omega_i|$ decreases with luminosity, because non-adiabaticity is stronger (or thermal time is shorter) in more luminous models. Conversely, as luminosity decreases, ω_r decreases and become essentially equal to zero at a certain luminosity for a given mass and α , below which the mode behaves as a monotonic g⁻ mode. This means that there is a minimum luminosity for the presence of oscillatory convective modes depending on the mass and α . The minimum luminosity is higher for larger mass for a given α , while it is higher for larger α for a given mass (Fig. 3). These dependences can be understood using the thermal time given in eq. (3) which should be inversely proportional to the strength of nonadiabaticity. For a larger mass model, a higher luminosity is needed to compensate a larger numerator, $M - M_r$, of eq. (3); the same is true for a model with larger α , because radius is smaller and hence mean density of the envelope is larger, which means that $M - M_r$ is larger for a given temperature.

As seen in Fig. 3, ω_r increases as luminosity increases and become nearly equal to the absolute value of the imaginary part, $|\omega_i|$, where each line is terminated. We have terminated the sequence because the amplitude in the radiative core becomes extremely large ($> 10^4$) and rapidly oscillating for a mode with $\omega_r \gtrsim |\omega_i|$, although the amplitude distribution in the envelope hardly differs from that shown in Fig. 2. Such a huge amplitude in the core is caused by a coupling with a high-order g-mode; i.e., the mode is a mixed mode consisting of an oscillatory convective mode in the outer envelope and high-order g mode in the core. It is not possible to resolve well such a large amplitude eigenfunction in the core (where $r/R < 10^{-4}$) with a few ten thousands mass shells we are using. In such a mode, it is expected that non-linear effects in the core would become significant before the surface amplitude becomes appreciable. For this reason we consider only pure oscillatory convective modes with $\omega_r \lesssim |\omega_i|$ to be observable.

Nonradial pulsations in a red giant are known to have mixed mode properties, with p-mode characteristics in the envelope and g-mode characteristics in the core (Dziembowski et al. 2001). The trapping of the p-mode in the envelope becomes very efficient as the luminosity increases as discussed by Dupret et al. (2009). However, the coupling between an oscillatory convective mode in the envelope and a core g-mode is different from the p- and g-mode coupling. In the case of the oscillatory convective mode, no isolation of the envelope oscillation from the core g-mode mode occurs if $\omega_r > |\omega_i|$; i.e., the amplitude of the coupled g-mode in the core is always exceedingly large. The difference comes from the absence of an evanescent zone in the case of an oscillatory convection mode, while in the p- and g-mode coupling there is a narrow evanescent zone that separates the p-mode propagating envelope from the g-mode propagating core. We note that the isolation of the oscillatory convective mode in the envelope does occur in helium shell flashing (thermal pulsing) models, in which a shell convection zone is present associated with the helium burning shell. The shell convection zone prevents the g-mode oscilla-

tion from propagating into the core just as in the blue supergiants SPB stars (Saio et al. 2006; Godart et al. 2009). We have not included such flashing models in this paper because the short time duration of shell flashing means such stars will be rare.

4 COMPARISON WITH OBSERVED LSP VARIABILITY

4.1 Period-luminosity relation

Fig. 4 compares period luminosity (PL) relations of red giants in the LMC with theoretical period-luminosity relations of oscillatory convection modes (circles) and radial pulsations (solid and dashed lines). Models with $\alpha = 1.9$ are shown in the left panel and models with $\alpha = 1.2$ are shown in the right panel. Our aim here is to match the periods of oscillatory convection modes with those of the LSPs belonging to sequence D while simultaneously matching the radial pulsation modes to sequence C (fundamental radial mode) and the shorter-period pulsation sequences. Period data (Soszyński et al. 2009) for red-giant variables were taken from the OGLE-III website (<http://ogle.astrouw.edu.pl/>). The luminosity of each star was obtained in the same way as for the sequence D stars shown in Fig. 1.

The pulsation period is proportional to $\sigma_r^{-1} \propto R^{1.5}/\omega_r$ (eq. 1). The PL relations for radial pulsations are roughly straight lines because ω_r of each mode does not vary much along the AGB evolution. In contrast, the PL relation of the oscillatory convective mode has a peculiar shape. It bends and becomes nearly horizontal in less luminous parts, having a minimum period and a minimum luminosity. (The maximum luminosity corresponds to the point where $\omega_r = |\omega_i|$ as discussed in the previous section.) The bending in the PL relation is caused by a rapid change in ω_r as a function of luminosity near the minimum luminosity (see Fig. 3). Around the minimum luminosity, small ω_r governs the PL relation; period decreases rapidly as luminosity increases due to an increase in ω_r . At a certain luminosity, however, the $R^{1.5}$ effect exceeds the ω_r effect so that the period starts to increase with luminosity (R).

For models with the mixing-length parameter $\alpha = 1.2$ (right panel of Fig. 4), the PL relation of the oscillatory convective modes above the ‘bend’ is consistent with sequence D i.e., periods, the gradient of the relation, and the lower luminosity bound of sequence D agree with models of $M \gtrsim 1.0 M_\odot$. However, these models are cooler than the red-giant sequence of the LMC in the HR diagram as seen in Fig. 1 and the radial mode periods, at least for masses less than $\sim 2M_\odot$, are longer than the observed periods.

For models with $\alpha = 1.9$ (left panel of Fig. 4), which best agree with the distribution of red giants on the HR diagram (Fig. 1) in the LMC and which provide a reasonable match between radial-mode periods and observed pulsation periods, the periods of oscillatory convective modes above the ‘bend’ are too short for sequence D by a factor of ~ 2 . Periods can cross sequence D only below the ‘bend’, for which $\omega_r < 0.5\omega_i$ (open circles). Also, models of $M \geq 1.0 M_\odot$ cannot explain the lowest part of the sequence D; the minimum luminosity for $1.0 M_\odot$ is $\log L/L_\odot \approx 3.3$, which is higher than the lower bound of the sequence D ($\log L/L_\odot \approx 2.8$).

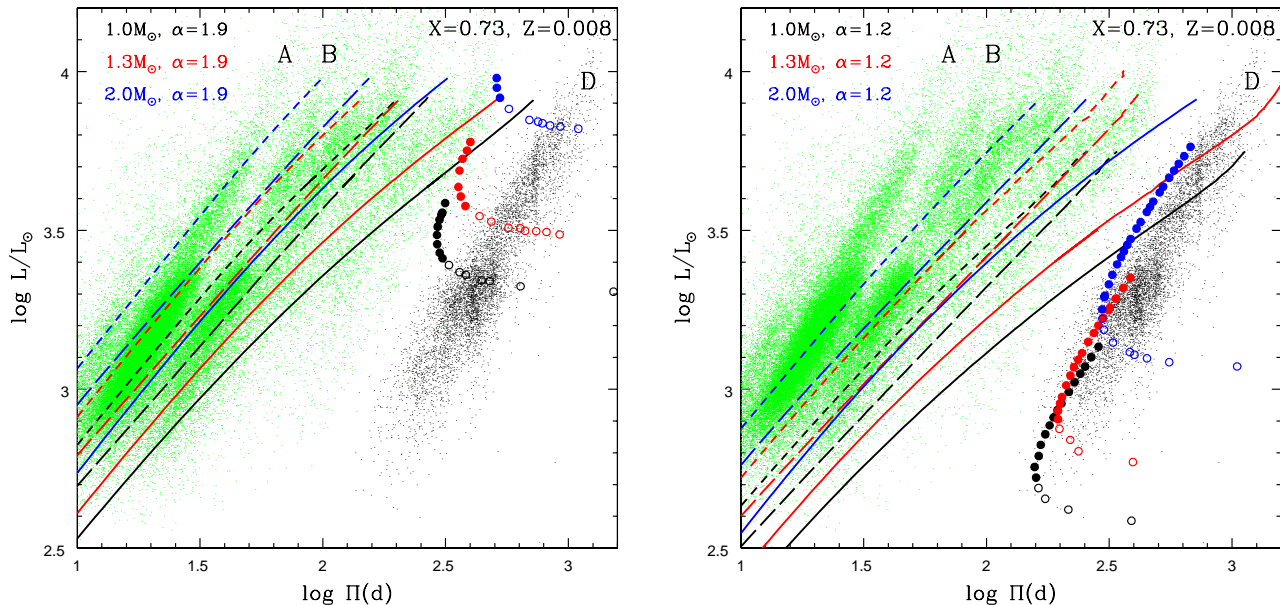


Figure 4. Period-luminosity relations of dipole oscillatory convective modes (circles) and radial modes in AGB models (non-flashing phases) with mixing length parameters of 1.9 (left) and 1.2 (right). Filled circles are for the modes with $\omega_r > 0.5|\omega_i|$ or vice versa for open circles. Solid lines, long dashed lines, and short dashed lines correspond to the radial fundamental, first overtone, and second overtone modes, respectively. A maximum luminosity of each period-luminosity relation for dipole oscillatory convective modes arises because in more luminous models coupling with a high-order g-mode in the core is significant and hence the amplitude in the core is extremely high. Also shown are red-giant variables in the LMC with LSPs on sequence D (small black dots) and pulsating red-giant variables with periods on sequences C, C', B and A (small green dots). The periods come from OGLE III (Soszyński et al. 2009).

Although the minimum luminosity for $\sim 0.8 M_\odot$ models decreases as low as the lower bound of the sequence D, the ages of these models exceed the cosmic age.

The problems in the $\alpha = 1.9$ models are caused, at least partially, by the weak nonadiabaticity. The strength of nonadiabatic effects in a convection zone depends on the distribution of density and temperature, which in turn depends on the convection model. In this paper, we have used the mixing-length theory, which is a poor approximation for the convection in luminous red-giants, and we have neglected turbulent pressure and possible overshooting. A better convection theory including turbulent pressure and possible overshooting might increase nonadiabatic effects significantly in outer layers, which could extend the luminosity range in which the oscillatory convective modes are found.

4.2 Phase relations

Fig. 5 shows predicted variations in luminosity, and photospheric density (top panels), temperature and radial displacements (bottom panels) as functions of pulsation phase of dipole ($\ell = 1$) modes for three $2 M_\odot$ models with different equilibrium luminosities; around the minimum period, middle, and the top of the PL sequence. The photospheric variations of $\delta T/T$, $\delta \rho/\rho$ and $\delta R/R$ were calculated using the eigenfunction at the mass shell corresponding to the photosphere in the equilibrium model, while $\delta L/L$ stands for the luminosity variation at the outer boundary which is located at an optical depth of 10^{-4} . We note that the quantities shown in Fig. 5 are not averaged across the surface

but are local values proportional to the spherical harmonic $Y_\ell^m(\theta, \phi)$. In particular, a dipole mode does not change the spherical shape and the mean radius of the stellar surface, although the local distance from the center of mass varies during pulsation. For this reason, we do not relate the observed radial velocity variation with a variation in the mean radius.

Fig. 5 shows that temperature is higher when density perturbation is negative (positive buoyancy) and radial displacement is positive for oscillatory convection modes. These phase relations are similar to those for normal convective instability, but are quite different from ordinary p- and g-modes. Because of the peculiar phase relations in oscillatory convective modes, temperature and luminosity are higher when radial displacement is positive. The amplitude of $\delta T/T$ relative to the radial displacement decreases with luminosity; the ratio is about 1.5 in a model at $\log L/L_\odot = 3.26$ (around the minimum period), while the ratio is reduced to about 0.2 at $\log L/L_\odot = 3.78$ (around the top of the PL relation). Non-adiabatic effects (thermal diffusion), which are stronger in more luminous models, reduce temperature variations. In addition, because of the stronger nonadiabatic effect, the phase relation between $\delta T/T$ and $\delta \rho/\rho$ shifts and the growth rate η decreases as the luminosity increases.

Fig. 6 shows systematic trends of the amplitude and phase of $\delta T/T$ and $\delta L/L$ as a function of luminosity for models of mass 2.0 (solid line), 1.3 (dashed line) and $1.0 M_\odot$ (dot-dashed line). The behaviour relative to the luminosity at minimum period (filled circles) is similar among the cases with different masses. For a given mass, as the luminosity

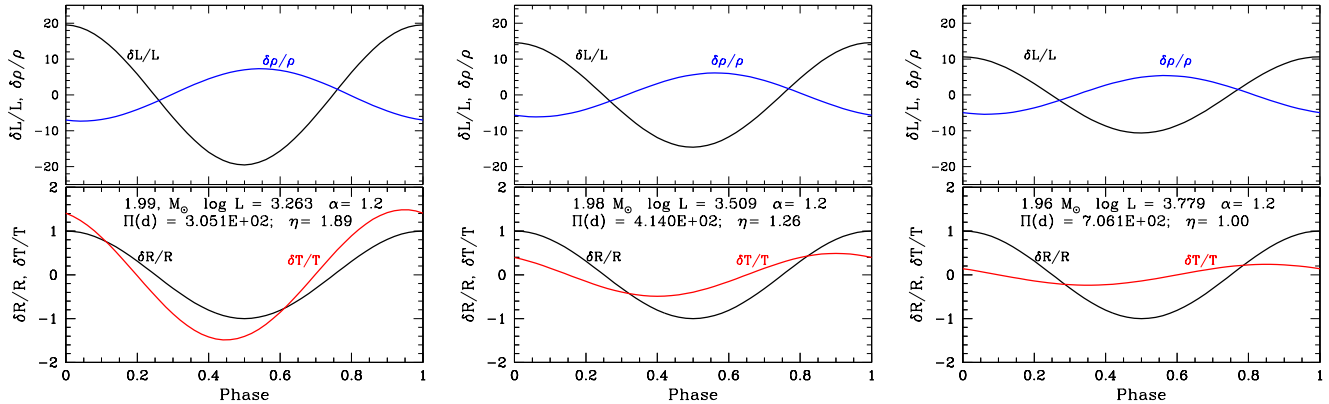


Figure 5. One cycle of the photospheric temperature variations, $\delta T/T$, radial displacements, $\delta R/R$ (bottom panels), and photospheric density variation, $\delta \rho/\rho$, and luminosity variation at the outer boundary, $\delta L/L$ (top panels) as a function of pulsation phase for dipole oscillatory convection modes in three models of $2.0 M_{\odot}$ ($\alpha = 1.2$) with different luminosities, where $\Pi(d)$ is period in days, and η is the growth rate defined as $-\omega_i/\omega_r$. The left panel is for a model around the minimum period (Fig. 4), the middle panel is for the same model as in Fig. 2, and the right panel is for a model close to the top of the period-luminosity relation in Fig. 4. The amplitude is normalized as $\delta R/R = 1$ at zero-phase, and is proportional to a spherical harmonic $Y_1^m(\theta, \phi)$ with θ and ϕ being co-latitude and azimuthal angle.

increases, the amplitudes of $\delta T/T$ and $\delta L/L$ decrease (relative to the amplitude of $\delta R/R$). The phase of $\delta T/T$ increases gradually with luminosity, while the phase of $\delta L/L$ stays very small (i.e. δL is in phase with δR). The phase difference between $\delta T/T$ (at photosphere) and $\delta L/L$ (at the outer boundary) arises because of the entropy variation between the photosphere and the outer boundary. The phase of the temperature variation at the outer boundary is very close to that of $\delta L/L$.

Nicholls et al. (2009) found various statistical properties of the LSP variability. They found that radius and temperature variations based on the radial velocity variations are very different from those determined from photometry or spectroscopic analysis (which would be expected if the pulsations are dipole modes). Here we summarize the properties of the majority of their sample based on photometric and spectroscopic analyses (i.e. we do not consider velocity data) as follows: (1) the phase delay of minimum light from the phase of minimum radius is mostly less than 0.2 period, (2) $\Delta T_{\text{eff}}/T_{\text{eff}} \lesssim 0.03$ and $\Delta R/R \sim 0.05$.¹

In the oscillatory convective modes shown in Fig. 5, minimum light occurs around minimum displacement which agrees reasonably well with the property (1). Because the pulsation is extremely nonadiabatic, temperature variation is very small. The ratio of the amplitudes of temperature and radius variations in the oscillatory convective mode ranges from about 2 to 0.2 (from around minimum period to the top of the sequence; see Figs. 5 and 6), while the property (2) above indicates the ratio is $\lesssim 0.6$ roughly consistent with the theoretical prediction. We note that if we use only photometric data, which cover all pulsation phases, the average of the whole sample is found around 0.23. Thus, the

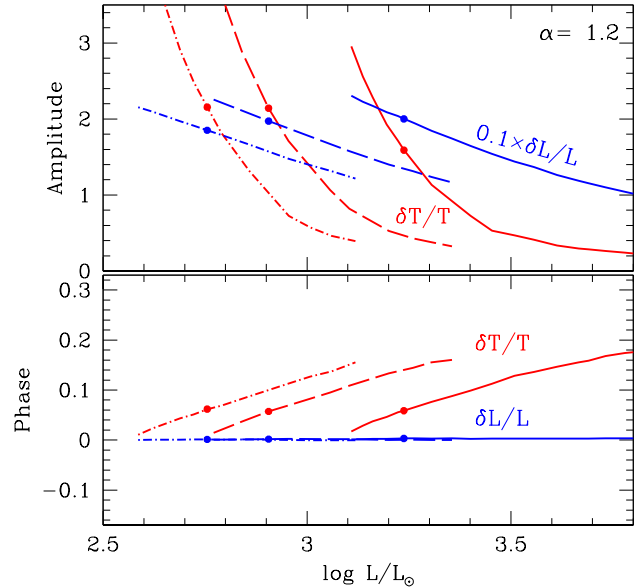


Figure 6. Amplitude (upper panel) and phase (lower panel) for the luminosity at the outer boundary (blue) and the photospheric temperature (red) variations of oscillatory convective modes ($\ell = 1$) versus luminosity. Solid, dashed, and dot-dashed lines are for 2.0 , 1.3 , and $1.0 M_{\odot}$ models, respectively. The amplitudes are normalized by the radial displacement, $\delta R/R$. The phase is in units of period, with zero phase corresponding to the phase of maximum $\delta R/R$. A filled circle indicates the position of the minimum period for each case.

¹ We note that although the whole surface averages of ΔT_{eff} and $\Delta R/R$ should be zero for nonradial pulsations, observational values should be non-zero because they correspond to the means across the visible hemisphere; the cancellation effect is smallest in dipole modes among nonradial pulsations.

properties of oscillatory convective modes seem consistent with the properties of the majority of the LSP sample of Nicholls et al. (2009).

Recently, Takayama, Wood & Ita (2015) examined color-magnitude variations during LSP variations for some

luminous SMC red giants. They found that matter should be ejected near the beginning of light decline. The matter might be related to the presence of chromosphere activity (Wood, Olivier & Kawaler 2004) and might be the origin of the excess mid-IR emission observed around stars with LSPs (Wood & Nicholls 2009). Fig. 5 indicates that maximum light occurs around maximum radial displacement, where mass ejection might be expected to occur. This is in agreement with phase of ejection found by Takayama, Wood & Ita (2015).

5 CONCLUSION

We discussed properties of the oscillatory convective modes in luminous red giants and compared them with the properties of the LSPs of variable red giants on the sequence D in the LMC.

The phase relations among temperature, radial displacement, and density variations in the oscillatory convective mode are similar to the relation expected for convective eddies rather than those of ordinary p- or g-modes; i.e., a positive temperature variation is associated with positive radial displacement and negative density variation. In addition, because of strong nonadiabatic effects the amplitude of the surface temperature variations is reduced relative to the radial displacement. These properties of the oscillatory convective mode roughly agree with the properties of the LSP variations of red giants in the LMC.

The period-luminosity relation of the oscillatory convective modes is found to be consistent with the observed relation of the LSPs of red-giants along sequence D if we adopt a mixing-length as small as 1.2 times pressure scale-height ($\alpha = 1.2$). However, these models are much cooler than the AGB stars in the LMC. For models with $\alpha = 1.9$, which agree with the effective temperatures of red giants in the LMC, periods are too short and the lower bound of the luminosity is too high, inconsistent with sequence D. Relatively weak nonadiabatic effect in the models with $\alpha = 1.9$ would cause, at least partially, the discrepancy. The shortcomings of the present models might be improved by employing a more sophisticated convection theory including turbulent pressure and possible overshooting. We leave the problem for future investigations.

ACKNOWLEDGEMENTS

We thank Bill Paxton and the MESA project team for developing the efficient stellar evolution code MESA. We also thank Marc-Antoine Dupret for constructive comments and suggestions as the referee of this paper.

REFERENCES

- Carpenter J. M., 2001, *AJ*, 121, 2851
 de Jager C., Nieuwenhuijzen H., van der Hucht K. A., 1988, *A&AS*, 72, 259
 Dupret M.-A. et al., 2009, *A&A*, 506, 57
 Dziembowski W. A., Gough D. O., Houdek G., Sienkiewicz R., 2001, *MNRAS*, 328, 601
 Dziembowski W. A., Soszyński I., 2010, *A&A*, 524, A88

- Godart M., Noels A., Dupret M.-A., Lebreton Y., 2009, *MNRAS*, 396, 1833
 Houdashelt M. L., Bell R. A., Sweigart A. V., 2000, *AJ*, 119, 1448
 Houdashelt M. L., Bell R. A., Sweigart A. V., Wing R. F., 2000, *AJ*, 119, 1424
 Ita Y. et al., 2004, *MNRAS*, 347, 720
 Keller S. C., Wood P. R., 2006, *ApJ*, 642, 834
 Kiss L. L., Bedding T. R., 2003, *MNRAS*, 343, L79
 Mosser B. et al., 2013, *A&A*, 559, A137
 Nicholls C. P., Wood P. R., Cioni M.-R. L., Soszyński I., 2009, *MNRAS*, 399, 2063
 Paxton B. et al., 2013, *ApJS*, 208, 4
 Saio H., 2011, *MNRAS*, 412, 1814
 Saio H., Cox J. P., 1980, *ApJ*, 236, 549
 Saio H. et al., 2006, *ApJ*, 650, 1111
 Shibahashi H., Osaki Y., 1981, *PASJ*, 33, 427
 Skrutskie M. F. et al., 2006, *AJ*, 131, 1163
 Soszyński I. et al., 2007, *AcA*, 57, 201
 Soszyński I., Udalski A., Kubiak M., Szymański M., Pietrzynski G., Żebruń K., Szewczyk O., Wyrzykowski L., 2004, *AcA*, 54, 129
 Soszyński I. et al., 2009, *AcA*, 59, 239
 Stothers R. B., 2010, *ApJ*, 725, 1170
 Takayama M., Saio H., Ita Y., 2013, *MNRAS*, 431, 3189
 Takayama M., Wood P. R., Ita Y., 2015, *MNRAS*, 448, 464
 Wood P. R., 2015, *MNRAS*, 448, 3829
 Wood P. R. et al., 1999, in *IAU Symposium*, Vol. 191, *Asymptotic Giant Branch Stars*, Le Bertre T., Lebre A., Waelkens C., eds., p. 151
 Wood P. R., Nicholls C. P., 2009, *ApJ*, 707, 573
 Wood P. R., Olivier E. A., Kawaler S. D., 2004, *ApJ*, 604, 800